Feature Article

Voltammetric Study of Methylene Blue at Thiol SAMs-Modified Gold Electrodes

Faqiong Zhao, Baizhao Zeng, Daiwen Pang*

Department of Chemistry, Wuhan University, Wuhan 430072, P.R. China
*e-mail: zengbz@chem.whu.edu.cn

Received: April 29, 2002
Final version: August 7, 2002

Abstract
The voltammetric behavior of methylene blue (MB) at thiol self-assembled monolayers modified gold electrodes (SAMs/Au) has been investigated. MB exhibited a redox peak at about -0.35 V (vs.SCE) in alkaline solution at bare gold electrodes. When the gold electrodes were modified with thiol SAMs, the peak grew due to the accumulation of MB at SAMs. With the solution pH rising, more MB was accumulated, hence the peak height increased, which differed from that at bare gold electrodes. The electrode process at SAMs/Au featured the characteristics of adsorption and/or electrode reaction controlled. The enhancing action of glutathione monolayer (GSH SAM), 3-mercaptopropionic acid monolayer (3MPA SAM) and other thiol SAMs was compared. Among these, GSH SAM made the MB peak increase more. At GSH SAM/Au, the peak height varied linearly with MB concentration over the range of 2 μM to 400 μM. So this can be developed for the determination of MB and studies concerned. The accumulation behavior caused by GSH SAM and native fish sperm dsDNA was compared. The interaction between DNA and MB was also discussed under this condition.

Keywords: Methylene blue, Thiols, Self-assembled monolayer, Gold electrode, DNA

1. Introduction

SAMs have been the subject of considerable interests in the last two decades due to their simple organizing procedure and regular orientation [1–4]. SAMs of various thickness, density and characteristics can be predesigned and prepared by varying the preparation procedure, self-assembling materials and so on. So far, they have been widely used in electroanalysis [3], electrocatalysis [5, 6], preparation of nano-meter material [7], and sometimes as the substrate for electrodeposition of metals [8, 9], mineral and polymer [10–13].

Monolayers of thiols formed at gold surface are a well-documented example of such so-called "self-assembled monolayers" because thiols easily form compact and organized monolayers through chemical adsorption. The function and property of the thiol SAMs can be improved by assembling two or more different thiol compounds simultaneously [14]. Thiol SAMs formed at gold surface have been extensively applied in electroanalysis as they can modify the electrode surface and make the electrodes show some new functions. They generally act as barriers to block the access of the redox species from the solution phrase to the electrode surface, sometimes as ion-gates, microarray electrodes or molecule/ion recognition bodies.

The blocking capability of thiol SAMs is related to the electroactive species, the thickness and compactness of the monolayer. In general, the electrode reaction can be blocked partly or completely by the SAMs [15]. For example, viologen, ferrocene and other organic dyes exhibited poorer redox waves at the *n*-dodecanethiol (C_{12}SH) SAM-modified gold electrodes than at bare gold electrodes. Their redox peaks were depressed and the peak potential separations (ΔE_p) were enlarged. In our experiment, the redox wave of $K_3Fe(CN)_6$ was almost invisible at C_{12}SH SAM/Au. However, in a few cases, SAMs played an active role in the electrochemical process and made the response of electroactive species greater. Sagara and his co-workers found that the electrode reaction of MB at C_{12}SH SAM/Au was facilitated under certain condition [16]. They thought that MB molecules partitioned into the C_{12}SH monolayer interior and the MB molecules were not in direct contact with the gold surface when the electron transfer took place. The C_{12}SH SAM acted not only as a barrier but also as an ultrathin medium for the redox reaction in this case. As we know, MB holds positive charges in solution, so its partition behavior must be affected by the solution pH and extra charges at the electrode surface. However, the influence of charges held by thiols and solution pH was not discussed in the literature. Our purpose is to explore the influence of the SAMs of different thiols and solution conditions on the electrochemical behavior of MB and to illustrate the reaction mechanism of MB at thiol SAMs/Au. In order to elucidate the interaction between GSH SAM and MB, the electrochemical behavior of MB at GSH SAM/Au and at dsDNA/Au was compared.

  1040-0397/03/1206-1060 $ 17.50+.50/0

2. Experimental

2.1. Chemicals

Native deoxyribonucleic acid (fish sperm) (dsDNA, Boao Biological Science Co., Shanghai, China) was used as received. Its stock solution was prepared by dissolving it in sterile double-distilled water. Methylene blue (3,7-bis (dimethylamino) phenothiazin-5-ium chloride, MB), purchased from the Third Chemical Factory of Shanghai, China, was recrystallized before use. 3-Mercaptopropionic acid (3MPA, >98% (HPLC), Fluka Co.), L-cysteine (L-cys, >99%, Caoyang Chemical Factory, Shanghai, China) and glutathione (GSH, Shanghai Yeast Factory, China) were used as received. All other chemicals were of reagent grade. Double-distilled water was used in this experiment.

2.2. Electrode Preparation

The polycrystalline gold electrode (>99.9%, 2.0 mm diameter, homemade, mounted in a Teflon rod) was polished to a mirror finish with alumina slurry of 0.3 μm and subsequently 0.05 μm, then rinsed thoroughly with water and ultrasonicated in a water bath to remove the embedded alumina particle. The electrode was examined by potential cycling in a 0.5 M KNO_3 solution containing 2 mM $K_3[Fe(CN)_6]$ between −0.2 V and 0.6 V until a constant voltammogram (typical of clean polycrystalline gold) was obtained. Afterward the electrode was rinsed with water and modified immediately by transferring a droplet of about 5 mg/mL dsDNA onto its surface followed by air-drying overnight. The electrode was then soaked in sterile water for at least 2 h and rinsed with water to remove the unadsorbed DNA. Thus the dsDNA-modified gold electrodes were obtained and denoted as dsDNA/Au in the text. If the dsDNA/Au was immersed into a thiol solution, a thiol SAM/dsDNA/Au could be obtained. The thiol SAMs modified gold electrodes were prepared using our previously described procedure [13]. Briefly, the cleaned Au electrode was immersed in a 0.05 M thiol aqueous solution for 12 h, then rinsed carefully with water and ultrasonicated in water for 5 s to remove the physical adsorbent. Similarly, when the thiol SAM/Au was further modified with fish sperm dsDNA, a new modified electrode represented as dsDNA/thiol SAM/Au was obtained.

2.3. Apparatus and Procedure

All electrochemical experiments were conducted with a CHI830 Electrochemical Analyzer (CH instrument Co., Shanghai, China) controlled by a personal computer in a single-compartment cell of 10 mL volume. A conventional three-electrode system was used. The bare gold electrode or modified gold electrode served as the working electrode, a saturated calomel electrode (SCE) and a platinum wire served as the reference and counter electrode, respectively. Cyclic voltammograms (CVs) were collected between −0.6 V and 0.3 V or in a narrower potential range. The peak height, peak area and peak potential were measured. The supporting electrolyte was a 40 mM sodium phosphate buffer unless stated elsewhere. The pH values were adjusted using HCl or NaOH aqueous solutions and measured with a Mettler Toledo pH meter. All experiments were carried out at room temperature.

3. Results and Discussion

3.1. Influence of Solution pH on the CVs of MB

Figure 1 shows the CVs of MB at different electrodes. MB exhibited a redox peak at about 0.1 V (i.e., formal potential) in acidic solutions at bare gold electrodes (Fig. 1A). The peak shifted negatively and the peak height changed slightly with increasing solution pH. This indicates that protons took part in the electrode reaction and the solution pH had little influence on the adsorption accumulation of MB [16]. As the peak potential/formal potential shifted more rapidly with pH changing in acidic solution than in basic solution, the proton number included in the electrode reaction may change with solution pH. At bare gold electrodes, ΔE_p was generally larger than 20 mV and the baseline was very steep. So the symmetry of the redox peak was poor and it was difficult to measure the anodic current value exactly under this condition.

At thiol SAMs/Au under investigation, the CVs of MB exhibited some different characteristics compared with those at bare gold electrodes. First, in most cases, the baseline became flatter and the peak shape was more symmetrical. This is due to the blocking action of SAMs, which partly minimized the background signal and hindered the redox reaction of other electroactives dissolved in the solution such as O_2. As the baseline also became flatter after the solution was purged by nitrogen gas, it was related to the dissolved oxygen and the SAMs can block the reduction of O_2. Second, the peak height and peak area increased, indicating more MB took part in the electrode reaction. This means that MB can be accumulated at the SAMs since there was no catalytic cycle included. It is known that SAMs usually act as a barrier and block the electrode reaction. In this case, however, it mainly acted as a medium in the interfacial redox reaction, which can accumulate MB and facilitate the electrode reaction as reported by Sagara [16]. As these thiols always turn to anion or cation in solution, thus the thiol SAMs also hold extra charges. Therefore, MB was accumulated through electrostatic attraction and incorporation of MB into the thiol SAMs, differing from its behavior at $C_{12}SH$ SAM/Au, at which MB was enriched mainly by incorporation. Because the peak height increased with pH rising and the SAMs held more negative charges in solutions with higher pH value, the electrostatic attraction between SAMs and MB must play an important role in the electrode process. It is worthwhile to note that the thiols used are hydrophilic and the hydrocarbon chains bearing

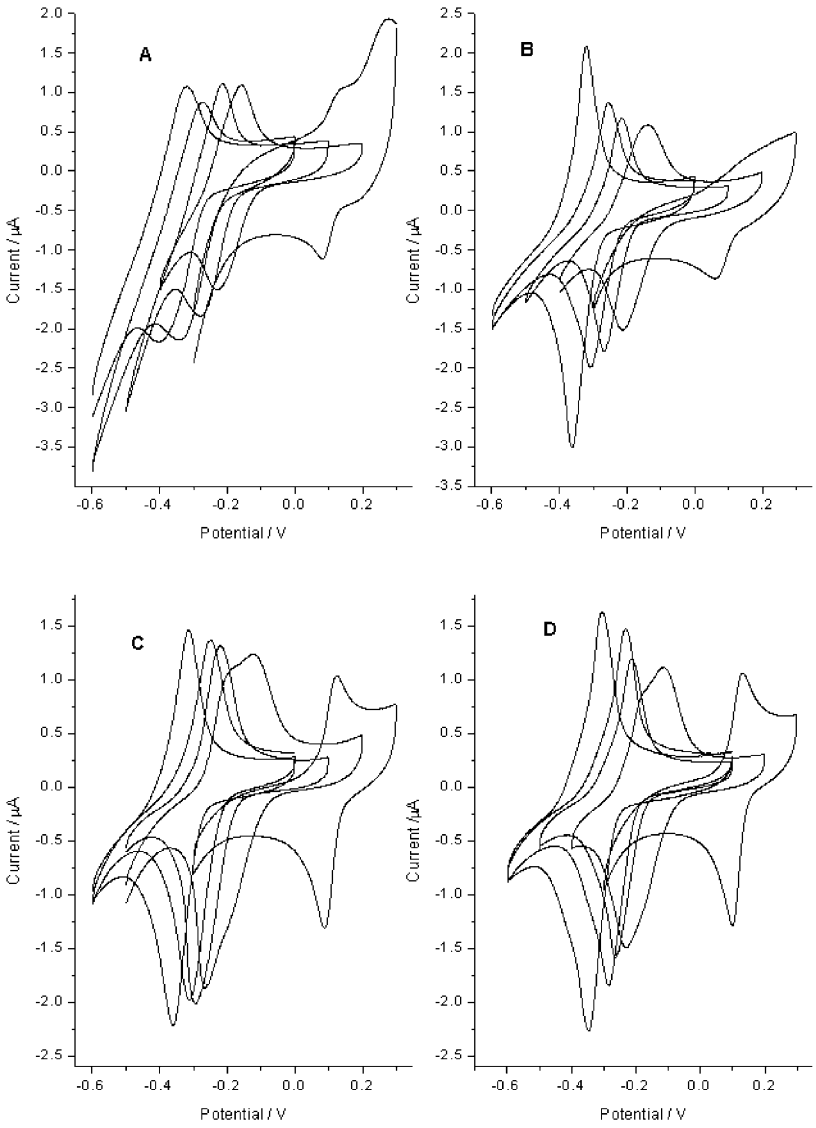

Fig. 1. Cyclic voltammograms (CVs) of 50 μM MB at bare gold electrode (A), GSH SAM/Au (B), 3MPA SAM/Au (C) and *N*-L-cys SAM/Au (D). Supporting electrolyte: 40 mM sodium phosphate buffer; solution pH: 12.1, 9.7, 7.1, 4.66, 1.6 (from left to right); scan rate: 100 mV/s.

are shorter, so the partition of MB into the films is weaker in comparison with long hydrocarbon chain thiols. In addition, varying the solution pH would cause the change of SAM property such as density, orientation and charge holding, resulting in the variation of accumulation amount of MB. In strong alkaline solutions, the peak was sharper and higher. Third, the peak potential was more positive than that at the bare gold electrode. This was also related to the interaction of MB with SAMs. Bard et al [17–19] reported in their article that hydrophobic interaction (i.e., intercalation) between the redox molecule and double-stranded DNA would lead to the formal potential shifting to positive while electrostatic interaction resulted in the formal potential shifting to negative. Here, the positive shift of the formal potential was thought to be caused by the ultrathin medium. It is the SAMs medium made the interfacial microenvironment change, and the potential energy of the MB thus varied, resulting in the change of the formal potential. Additionally, the ΔE_p became smaller, illustrating the reversibility improved at thiol SAMs/Au.

Figure 1 (B, C and D) shows the influence of solution pH on the CVs of 50 μM MB at GSH, 3MPA and *N*-acetyl-L-cysteine (*N*-L-cys) SAM/Au, respectively. Different enhancing effect on the current peak can be observed. This results from the differences among their molecular structure and dissociation constants (*Ka*), which are related to the accumulation capability and surface charges of thiol SAMs/Au. Although thiols self-assembled on the electrode surface show greater *Ka* than in solution [20], their *Ka* generally follow the same order as in solution. In this case, their *Ka* and hydrocarbon chains were still thought to follow such order as: *Ka* (3MPA) ≈ *Ka* (*N*-L-cys) > *Ka* (GSH); C_5

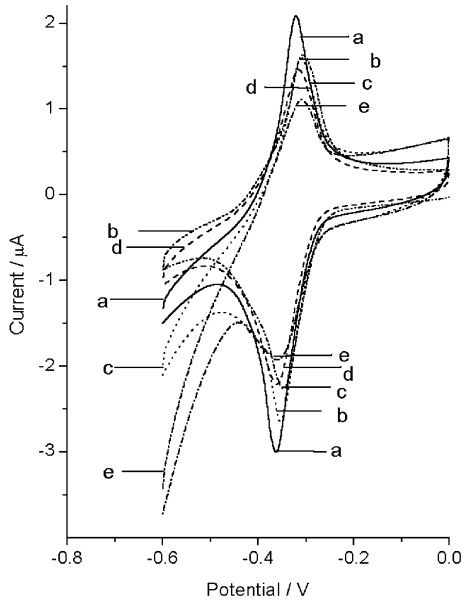

Fig. 2. CVs of 50 μM MB at GSH SAM/Au (a), *N*-L-cys SAM/Au(b), L-cys SAM/Au(c), 3MPA SAM/ Au(d) and L-cysteamine SAM/Au(e). Solution pH: 12.1; other conditions as in Figure 1.

(GSH) > C_4 (*N*-L-cys) > C_3 (3MPA). Accordingly the electrostatic attraction between MB and SAMs/Au reached the maximum at lower pH for 3MPA SAM/Au and at higher pH for GSH SAM/Au. The peak height almost kept unchanged for 3MPA SAM/Au when pH exceeded 5, where it fully dissociated. However, for *N*-L-cys and GSH, the peaks grew with pH rising all the time, indicating that the pH can affect the MB peak through other way in addition to varying the electrostatic interaction. As mentioned above, the characteristics (i.e., monolayer structure, compact and orientation) of SAMs depended on the solution pH, so the accumulation capability and enhancing effect of SAMs changed with pH. Although the density and thickness of SAM also influenced the electrochemical behavior and accumulation of MB, in this case, the electrostatic attraction/repulsion was thought to dominate over the incorporation/partition of MB into SAM layer because the SAMs prepared with short chain alkanethiols and peptides were relative thin and contained many pinholes. Therefore the higher affinity with GSH and *N*-L-cys over 3MPA indicated that the amine on each was involved in complexing the MB as well as the electrostatic attraction of the carboxylate. It is worth noting that two overlapped peaks could be observed sometime (Fig. 1B, C and D, pH 4.66). This should be ascribed to the two successive 1e – transfer electrode reactions, which caused two peaks. The peaks overlapped at about pH 4 and completely merged at other pH values.

For comparison, the CVs of MB in pH 12.1 sodium phosphate buffer are shown in Figure 2. Among these, MB exhibited the greatest peak current at GSH SAM/Au. So GSH SAM/Au was more suitable for the determination of MB. When MB concentration reduced down to 10 μM, the enhancing effect was still visible at thiol SAMs/Au (except at

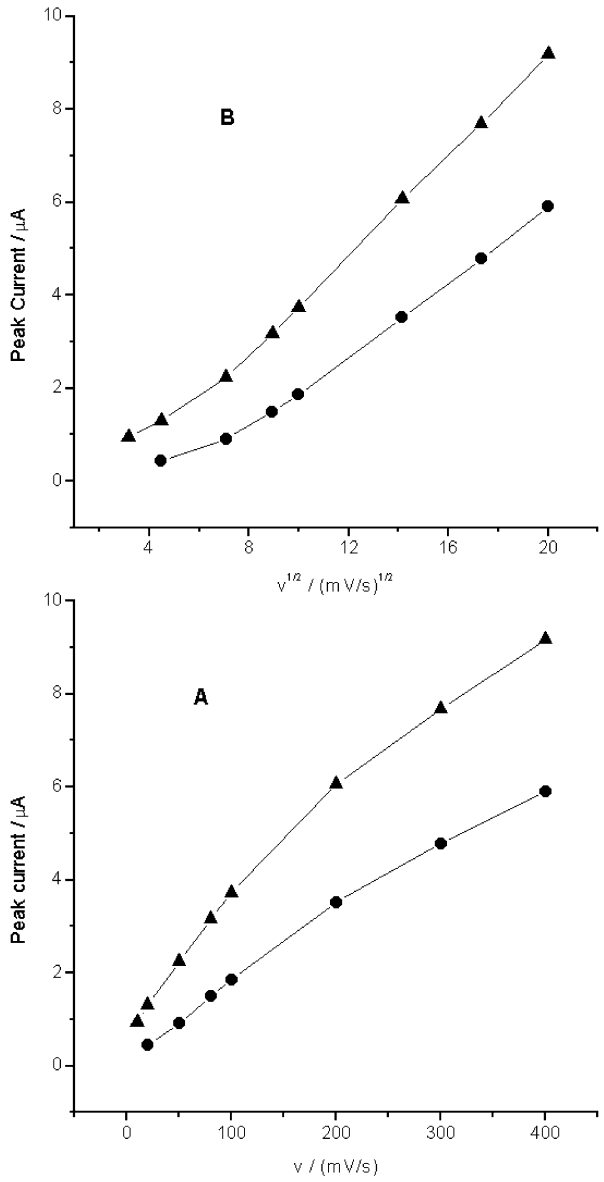

Fig. 3. Dependence of the anodic peak current (●) and cathodic peak current (▲) on scan rate (A) and its square root (B). Solution pH: 12.1; other conditions as in Figure 1.

L-cystamine SAM/Au), especially at GSH SAM/Au and 3MPA SAM/Au. When the MB concentration reduced to 5 μM, the CVs of MB at L-cys SAM/Au, L-cysteamine SAM/Au and 3MPA SAM/Au were distorted and small change occurred compared with those obtained at the bare gold electrode. But at GSH/Au and *N*-L-cys/Au, CVs with sharper redox peaks for MB still can be obtained.

3.2. Dependence of the Peak Height on the Scan Rate (*v*)

The dependence of the peak height on the scan rate has been studied (Fig. 3). In pH 12.1 solutions, the redox peak (whether the cathodic or anodic peak) height varied linearly with scan rate over the range of 0 to 200 mV/s. When it was

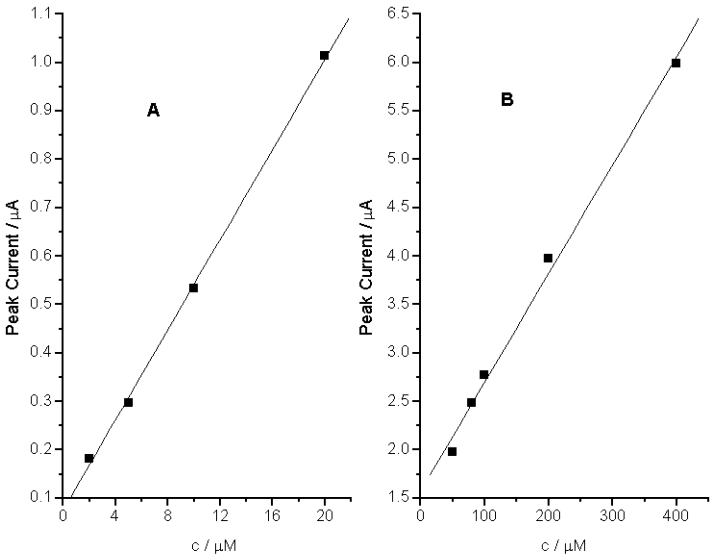

Fig. 4. Dependence of the anodic peak current on MB concentration. Solution pH: 7.1; other conditions as in Figure 1.

over 200 mV/s, the $i_p - v$ plot slightly turned to abscissas. It seems that the electrochemical process was adsorption-controlled at lower scan rate and was not at higher scan rate. With scan rate rising, the peak potential separation (ΔE_p) increased, revealing the electrode reaction became less reversible at higher scan rate and the electron transfer rate was not great enough. On the other hand, the MB concentration was small and the diffusion current did not dominate over the adsorption current as discussed below. Therefore, it was thought that the electrochemical process was electrode reaction controlled or mix-controlled at higher scan rate. In neutral buffer, the phenomenon was similar to that in alkaline solutions.

3.3. Influence of Accumulation on the CVs of MB

In this experiment, it was found that an open circuit accumulation made the peak height increase, which can be ascribed to the incorporation of MB into the thiol SAMs and the electrostatic attraction. In pH 12.1 alkaline solutions, an open circuit accumulation of 10 min made the anodic peak current (i_{pa}) increase by 224% and the cathodic one (i_{pc}) increase by 104% for 10 μM MB, respectively. But for a 50 μM MB, they only increased by 4.9% and 6.6% respectively. However, an accumulation at certain potential would make the peak height decrease, e.g., for 50 μM MB, a 10 min accumulation at -0.6 V made the i_{pa} decrease by 56% and i_{pc} by 31% in pH 12.1 solutions; a 3 min accumulation at -0.2 V made i_{pa} and i_{pc} reduce by 28.5% and 21.2% respectively. This differs from the phenomenon observed by Sagara at $C_{12}SH$ SAM. It was explained as the thiol SAMs mentioned above were not dense enough and the accumulation potential weakened the electrostatic interaction and affected the surface structure partly, so it hindered the adsorption and/or incorporation of MB at the SAMs.

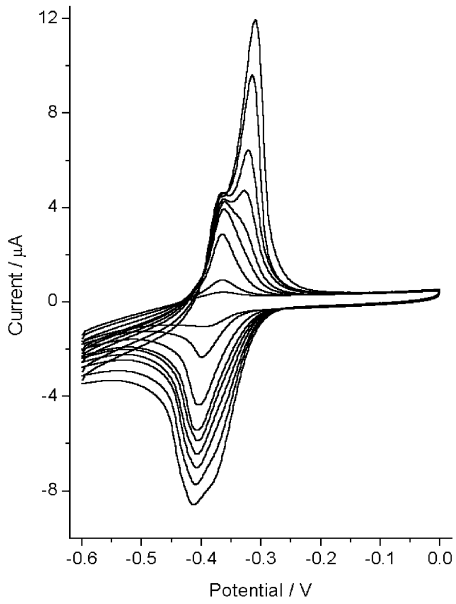

Fig. 5. Variation of the CV with MB concentration. MB concentration (from internal to external): 10, 20, 50, 80, 100, 200, 300 and 400 μM; solution pH: 12.1; other conditions as in Figure 1.

3.4. Dependence of the Peak Height on MB Concentration

Figures 4 and 5 show the CV response of MB at various concentrations and the linear relationship between the peak current and MB concentration. As can be seen, MB exhibited a well-defined redox peak within small concentration range. When its concentration was over 100 μM, the anodic peak broadened (Fig. 5). This was mainly due to the increase of diffusion-controlled current, which had more positive formal potential [16]. When the MB concentration

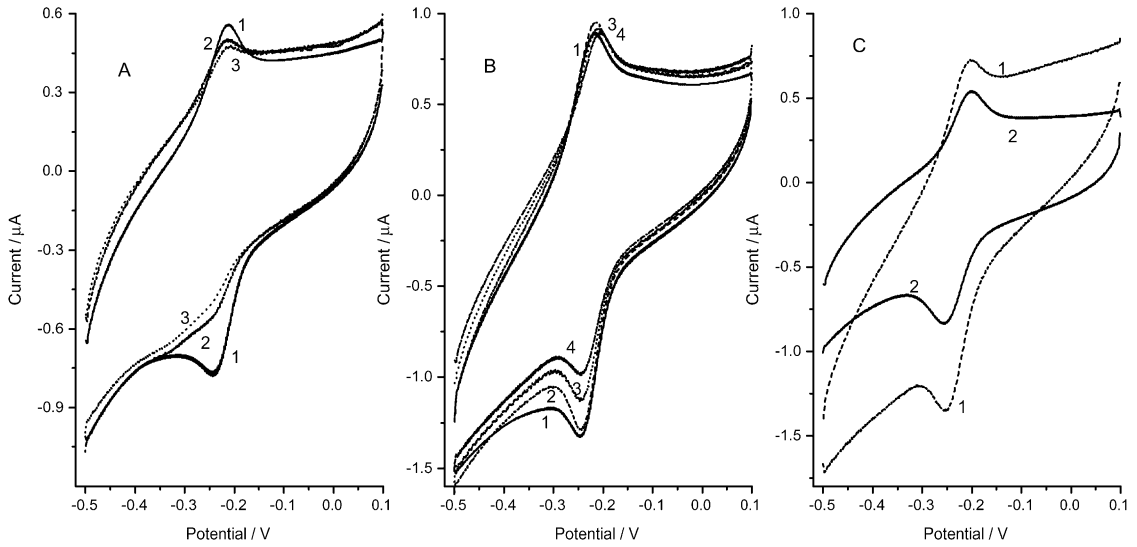

Fig. 6. CVs of 10 μM MB at GSH SAM/Au (A), dsDNA/Au (B), GSH SAM/dsDNA/Au (C1) and dsDNA/GSH SAM/Au (C2). For A the solutions contained 0, 83, 166 μg/mL native sperm DNA (A1 to A3); for B the solutions contained 0, 0.4, 1.2, 2.0 mM GSH (B1 to B4) respectively. Supporting electrolyte: 40 mM phosphate buffer (pH 6.84); other conditions as in Figure 1.

was further increased, the anodic peak at about -0.32 V shifted slightly toward positive direction and the peak current increased significantly, but the anodic peak at about -0.37 V changed slightly, which was similar to that observed at a mercury electrode [21]. This also indicated that the peak, which appeared only in solutions with high MB concentration, was caused by the diffusing of MB in solution. The peak at about -0.37 V was generated by the adsorbed/confined MB molecules, whose peak current changed slightly when MB concentration was increased, because a saturated adsorption was achieved under this condition. Additionally, higher MB concentration could lead to the distorting of the cathodic peak in alkaline or neutral solutions. It is clear that the baseline of the negative scan was flatter than that of the positive scan, so it was more convenient to measure the cathodic peak current. As shown in Figure 4 the cathodic peak current was linear to MB concentration over the range of 2 μM to 20 μM and 50 μM to 400 μM with slopes of 0.047 μA/μM ($r=0.9995$) and 0.011 μA/μM ($r=0.997$), respectively. Because the SAMs blocked the access of some redox species, the detection of MB suffered less interference from other coexistent.

3.5. Comparison of the Electrochemical Behavior of MB at GSH SAM/Au and dsDNA/Au

It is well known that MB is an aromatic heterocycle that binds to dsDNA mainly via intercalation [22–24]. Figure 6B1 shows the CV of MB in neutral phosphate buffer. Although the MB concentration was very low (10 μM), a rather strong response can be obtained, which differed from that observed by Ozsoz at carbon paste electrodes (CPE) [23]. They found the MB amount accumulated at dsDNA modified CPE reduced compared with at bare CPE. Part of the reason was that the phenothiazine compounds were more easily adsorbed at CPE than at bare gold electrode. Under the same condition, only a very small redox peak could be obtained at the bare gold electrode. The response at dsDNA/Au was similar to that at GSH SAM/Au (Fig. 6A), but the peak height of MB was always greater at dsDNA/Au. In order to examine the binding strength between MB and GSH, dsDNA was introduced. Figure 6A shows the CVs of MB at GSH SAM/Au in MB solutions containing dsDNA. It is clear that in the presence of dsDNA, the redox peak was depressed, especially the cathodic one. This indicated that the MB preferentially bound to DNA in solution and the resulting complex cannot be accumulated effectively at the GSH SAM/Au like MB due to the electrostatic repulse and steric hindrance. The preference for MB to bind with DNA over GSH could be illustrated by the lower peak separation of MB when interacting with the DNA rather than the GSH. Such binding also made the partition of MB into the GSH SAM difficult and the mass-transfer slow. The influence of GSH on the electrochemical behavior of MB at dsDNA/Au was investigated. As Figure 6B shows, in sodium phosphate buffer, with the addition of GSH, the redox peak first increased slightly then decreased a little. The slight decrease in MB signal reflected the GSH displacing some of the DNA from the electrode surface because the DNA was immobilized on the electrode surface by non-specially adsorption. The cathodic peak potential remained constant at -0.246 V, while the anodic one shifted to positive slightly.

To give a more comprehensive comparison, the electrochemical behavior of MB at GSH SAM/dsDNA/Au and dsDNA/GSH SAM/Au was further studied (Fig. 6C). It can be concluded that dsDNA/GSH SAM/Au can make the baseline flatter and the redox peak more symmetrical, while MB at GSH SAM/dsDNA/Au shows smaller ΔE_p, indicating

a more reversible electrochemical process. In the GSH SAM/dsDNA/Au case, the GSH added afterwards would fill the gaps between the DNA and perhaps displace some DNA as discussed above. So the DNA appeared to be in direct contact with the electrode. In the dsDNA/GSH SAM/Au case, the electrode was first coated with GSH and then the DNA would be expected to adsorb onto the GSH layer. So in the latter case the DNA may not be directly in contact the electrode as it was unlikely to displace the GSH. This was shown clearly in the CVs by the lower double layer capacitance in this latter case. It is worth noting that the CVs at GSH SAM/dsDNA/Au and dsDNA/GSH SAM//Au were quite different from at either dsDNA/Au or GSH SAM/Au. The ΔE_p at the former was far greater than at the latter (i.e., > 50 mV at the former, about 30 mV at the latter), indicating the second monolayer was self-assembled at the first monolayer differing from it at the bare gold electrode, and the electron transfer was blocked partly by the thick film formed on the gold electrode.

4. Conclusions

GSH, 3MPA and *N*-L-cys SAMs can accumulate MB and facilitate the electrode reaction of MB, hence they can improve the CV response of MB to some degree. This differs from that SAMs usually exert block action to electrochemical process of electroactive molecules such as $K_3Fe(CN)_6$ and ferrocene. The enhancing effect grows with solution pH rising, MB thus exhibits a sensitive redox peak suitable for its determination in neutral and alkaline solutions. Such system can be used to explore the interaction of MB with DNA and mechanism concerned.

5. Acknowledgement

The authors appreciate the financial support provided by the Electroanalytical Chemistry Lab of Application Chemistry Institute of Changchun, China.

6. References

[1] J. D. Swalen, D. L. Allara, J. D. Andrade, E. A. Chandross, S. Garoff, J. Israelachvili, T. J. McCarthy, R. Murray, R. F. Pease, J. F. Rabolt, K. J. Wynne, H. Yu, *Langmuir* **1987**, *3*, 932.
[2] J. Wang, B-Z. Zeng, C. Fang, X-Y. Zhou, *Anal. Sci.* **2000**, *16*, 457.
[3] F. Malem, D. Mandler, *Anal. Chem.* **1993**, *65*, 37.
[4] L. Häussling, H. Ringsdorf, *Langmuir* **1991**, *7*, 1837.
[5] M. Ohtani, S. Kuwabata, H. Yoneyama, *J. Electroanal. Chem.* **1997**, *422*, 45.
[6] D. Dicu, L. Muresan, I. C. Popescu, C. Cristea, I. A. Silberg, P. Brouant, *Electrochim. Acta* **2000**, *45*, 3951.
[7] X. Chen, J. Jing, W-S. Yang, *Chem. J. Chinese Univ.* **2000**, *21*, 1115.
[8] J. K. Schoer, C. B. Ross, R. M. Crook, T. S. Corbitt, M. J. Hampdensmith, *Langmuir* **1994**, *10*, 615.
[9] S. J. Potochnik, P. E. Pehrsson, D. S. Y. Hsu, J. M. Calvert, *Langmuir* **1995**, *11*, 1841.
[10] P. C. Pieke, B. J. Tarasevich, L. L. Wood, M. H. Engelhard, D. R. Beaar, G. E. Fryxell, C. M. John, D. A. Laken, M. C. Jaehning, *Langmuir* **1994**, *10*, 619.
[11] H. Yoneyama, M. Kitayama, *Chem. Lett.* **1986**, *5*, 657.
[12] M. Okano, E. Kikuchi, K. Itoh, A. Fujishima, *J. Electrochem. Soc.* **1988**, *135*, 1641.
[13] B-Z. Zeng, F-Q. Zhao, X-G. Ding, *Anal. Sci.* **2001**, *17*, 259.
[14] J. Wang, B-Z. Zeng, C. Fang, X-Y. Zhou, *Electroanalysis* **2000**, *12*, 763.
[15] J. Wang, B-Z. Zeng, C. Fang, F. He, X-Y. Zhou, *Electroanalysis* **1999**, *11*, 1345.
[16] T. Sagara, H. Kawamura, N. Nakashima, *Langmuir* **1996**, *12*, 4253.
[17] M. T. Carter, A. J. Bard, *J. Am. Chem. Soc.* **1987**, *109*, 7528.
[18] M. T. Carter, M. Rodoriguez, A. J. Bard, *J. Am. Chem. Soc.* **1989**, *111*, 8901.
[19] M. Rodoriguez, A. J. Bard, *Anal. Chem.* **1990**, *62*, 2658.
[20] J-W. Zhao, L-Q. Luo, X-Y. Yang, E-K. Wang, S-J. Dong, *Electroanalysis* **1999**, *11*, 1108.
[21] R. H. Wopschall, I. Shain, *Anal. Chem.* **1967**, *39*, 1527.
[22] G-C. Zhao, J-J. Zhu, J-J. Zhang, H-Y. Chen, *Anal. Chim. Acta* **1999**, *394*, 337.
[23] E. M. Tuite, J. M. Kelley, *J. Photochem. Photobiol.* **1993**, *21*, 103.
[24] A. Erdem, K. Kerman, B. Meric, U. S. Akarca, M. Ozsoz, *Anal. Chim. Acta* **2000**, *422*, 139.